

Naphthoquinone–Dopamine Hybrids Inhibit α-Synuclein Aggregation, Disrupt Preformed Fibrils, and Attenuate Aggregate-Induced Toxicity

Ashim Paul, Adi Huber, Daniel Rand, Fabien Gosselet, Itzik Cooper, Ehud Gazit, Daniel Segal

▶ **To cite this version:**

Ashim Paul, Adi Huber, Daniel Rand, Fabien Gosselet, Itzik Cooper, et al.. Naphthoquinone–Dopamine Hybrids Inhibit α-Synuclein Aggregation, Disrupt Preformed Fibrils, and Attenuate Aggregate-Induced Toxicity. Chemistry - A European Journal, 2020, 26 (69), pp.16486-16496. 10.1002/chem.202003374 . hal-03126960

HAL Id: hal-03126960

https://univ-artois.hal.science/hal-03126960

Submitted on 19 Jul 2022

HAL is a multi-disciplinary open access archive for the deposit and dissemination of scientific research documents, whether they are published or not. The documents may come from teaching and research institutions in France or abroad, or from public or private research centers.

L'archive ouverte pluridisciplinaire **HAL**, est destinée au dépôt et à la diffusion de documents scientifiques de niveau recherche, publiés ou non, émanant des établissements d'enseignement et de recherche français ou étrangers, des laboratoires publics ou privés.

Naphthoquinone-Dopamine hybrids inhibit α-synuclein aggregation, disrupt preformed fibrils and attenuate aggregate-induced toxicity

Ashim Paul,[1] Adi Huber,[1] Daniel Rand,[2] Fabien Gosselet,[3] Itzik Cooper,[2] Ehud Gazit[1,4] and Daniel Segal[1,5]*

[1]Department of Molecular Microbiology and Biotechnology, School of Molecular Cell Biology and Biotechnology, Tel Aviv University, Ramat Aviv, Tel Aviv 6997801, Israel.

[2]The Joseph Sagol Neuroscience Center, Sheba Medical Center, Tel Hashomer, Ramat Gan 52621, Israel.

[3]Artois University, UR 2465, Blood-brain barrier Laboratory (LBHE), F-62300 Lens, France.

[4]Department of Materials Science and Engineering, Iby and Aladar Fleischman Faculty of Engineering, Tel Aviv University, Ramat Aviv, Tel Aviv 6997801, Israel.

[5]Sagol Interdisciplinary School of Neuroscience, Tel Aviv University, Ramat Aviv, Tel Aviv 6997801, Israel.

[*]Corresponding to:

Daniel Segal

Department of Molecular Microbiology and Biotechnology, School of Molecular Cell Biology and Biotechnology, Tel Aviv University, Ramat Aviv, Tel Aviv 6997801, Israel

E-mail: dsegal@post.tau.ac.il

phone: ++972-3-640-9835

fax: ++972-3-640-9407

Abstract

Accumulation and aggregation of the intrinsically disordered protein α-synuclein (α-Syn) into amyloid fibrils are hallmarks of a series of heterogeneous neurodegenerative disorders, known as synucleinopathies and most notably Parkinson's disease (PD). The crucial role of α-Syn aggregation in PD makes it an attractive target for the development of disease-modifying therapeutics that would inhibit α-Syn aggregation or disrupt its preformed fibrillar assemblies. To that end, we have designed and synthesized two naphthoquinone-dopamine-based hybrid small molecules, NQDA and Cl-NQDA, and demonstrated their ability to inhibit in vitro amyloid formation by α-Syn using ThT assay, CD, TEM, and Congo red birefringence. Moreover, these hybrid molecules efficiently disassembled preformed fibrils of α-Syn into non-toxic species, as evident from LUV leakage assay. NQDA and Cl-NQDA were found to have low cytotoxicity and they attenuated the toxicity induced by α-Syn towards SH-SY5Y neuroblastoma cells. NQDA was found to efficiently cross an *in vitro* human blood-brain barrier model. These naphthoquinone-dopamine based derivatives can be an attractive scaffold for therapeutic design towards PD.

Keywords: Parkinson's disease, α-Syn, Aggregation, Inhibition, Disruption.

Introduction

Accumulation and aggregation of the protein α-synuclein (α-Syn) into oligomers and mature fibrils are key pathogenic characteristics of a series of heterogeneous neurodegenerative disorders, collectively termed synucleinopathies.[1–3] Parkinson's disease (PD), one of the most common synucleopathies, is a progressive neurodegenerative disorder, characterized by the loss of dopaminergic neurons and motor impairment including bradykinesia, muscular rigidity, and resting tremor.[3–6] Crucial steps in the initiation of PD are believed to be the misfolding of α-Syn and its consequent self-assembly into toxic oligomers that subsequently form insoluble amyloid fibrils which are deposited as Lewy Bodies in vulnerable regions of the brain, ultimately causing their demise.[5,7] The complex structural features of the intrinsically disordered unfolded α-Syn protein have made it difficult to elucidate the mechanism of its self-assembly into various isoforms, and the processes by which they trigger neuronal death are poorly understood.[6] However, a growing body of evidence suggests that the soluble aggregates of α-Syn, known as oligomers and protofibrils, are the major toxic species that interact with various cellular targets in the brain, leading to PD etiology.[8] Therefore, removal of these α-Syn aggregates or inhibition of their formation could be an attractive strategy for the development of disease-modifying therapeutics.

The primary structure of α-Syn comprises of three main regions: the N-terminus region (1-60 amino acids), the central core region (61–95 amino acids) also known as non-amyloid-β component (NAC), which forms the structural core of the amyloid fibrils,[9,10] and the C-terminal region (96–140 amino acids).[11] In aqueous solution, α-Syn remains unfolded, while in a lipid environment it folds into α-helical conformation, and was suggested to exist helical tetramers in the cytoplasm. In diseased conditions, α-Syn misfolds into highly ordered β-sheet structures which self-assemble, leading to the formation of fibrillar aggregates.[9]

Various modulators have been designed and tested for pharmacological targeting of α-Syn including molecular chaperones,[12–14] antibodies,[15–17] synthetic peptides,[18–20] polydopamine dendrimers,[21] molecular tweezer,[22] and various small molecules or chemical chaperones.[23–27] Among them, antibody-based strategy has gained acclaim, despite their considerable production cost, due to their high specificity towards their targets.[16,17,28] Yet, raising antibodies against targets such as amyloidogenic proteins, certain membrane proteins, proteins within highly homologous families, and epitopes that agonize or antagonize a biological pathway, is challenging.[29,30] Small molecules, on the other hand, are preferred from the pharmacological perspective as they are of low molecular weight, high efficacy towards their target, and their cost is relatively low. Also, small molecules found to be

effective in targeting the monomeric protein as well as to the aggregates and shown potential activity in animal models of PD, and some of them have already entered into clinical trials.[31–34]

Here, we have developed dopamine-based molecules for targeting α-Syn, by combining dopamine (DA) with the naphthoquinone (NQ) molecule to obtain their hybrids, termed as NQDA and Cl-NQDA (Figure 1). DA is found in the brain and plays several important biological roles, including as hormone and neurotransmitter.[35,36] Its production and homeostasis in neurons is regulated by α-Syn through the interaction with tyrosine hydroxylase. DA was reported to form adducts with α-Syn *in vitro*, which stabilize the α-Syn protofibrils and inhibit its fibril formation, and certain DA derivatives alleviated α-Syn engendered defects in an animal model of PD .[37–41] Recently DA-modified α-Syn was found to block chaperone-mediated autophagy.[42] The other element of the designed hybrid molecules, NQ, was chosen because quinone exhibit various biological properties and its derivatives, for example NQTrp, were shown to modulate aggregation of several amyloidogenic proteins associated with various proteinopathies including PD.[27,43,44] The mode of action of NQTrp with an amyloidogenic protein likely occurs through π-π interaction between the aromatic moiety of Tryptophan and aromatic amino acid of the protein, while the quinone element interferes with the process aggregation, thus resulting in inhibition of amyloid formation.[44–47]

These activities of NQ derivatives and DA, prompted us to conjugate them and we hypothesized that the aromatic moiety of DA in the hybrid molecules NQDA and Cl-NQDA will bind the aromatic residues of α-Syn and intercalate within the β-sheets of the protein, whereas the NQ moiety together with the two hydroxyl groups of DA will hinder the α-Syn self-aggregation process to inhibit amyloid formation. A previous report, observed that Tyramine, which differs from DA only by a hydrogen replacing a hydroxyl group, exhibited less inhibitory activity than DA towards in α-Syn due to a loss of electrostatic interactions with the two negatively charged groups of the NAC region in α-Syn.[48] We reasoned that the π-electron-rich aromatic moiety of DA may intercalate the β-sheets of amyloid formed by α-Syn through the interaction with the aromatic residues, mainly at the Phe residue within the central hydrophobic NAC region through π- π interaction.

Using various *in vitro* methods, including Thioflavin T assay (ThT), Circular dichroism (CD) and Transmission electron microscopy (TEM) we demonstrate here that the hybrid molecules efficiently inhibit the aggregation of α-Syn and disrupt its preformed fibrils into non-toxic species. These novel dopamine-based hybrids can be used as a scaffold for novel therapeutics for PD.

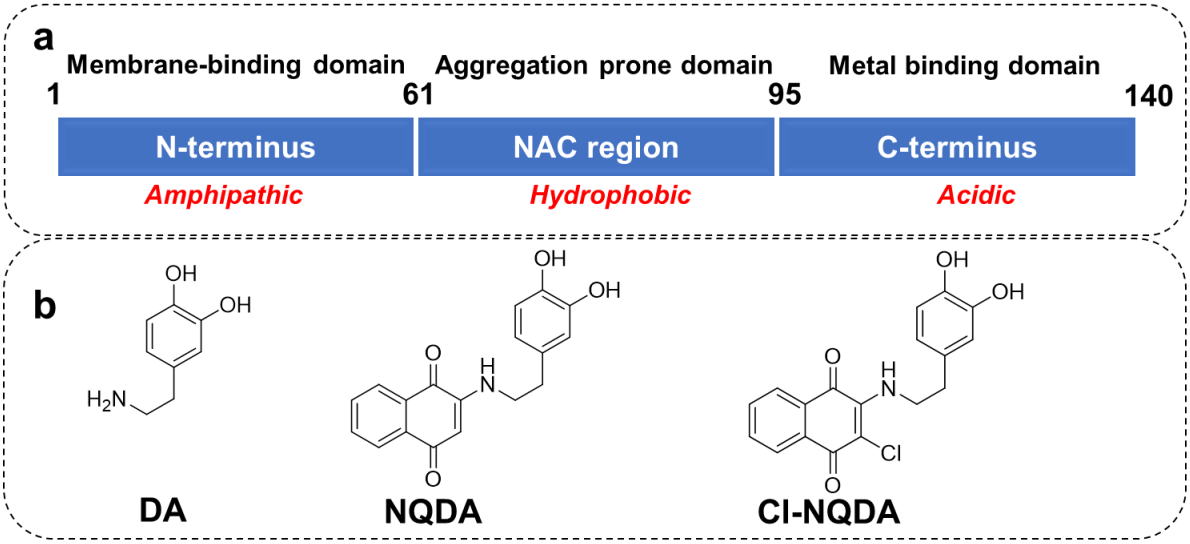


Figure 1. (a) Schematic structure of α-Syn. (b) Chemical structures of DA, NQDA and Cl-NQDA.

Results and Discussion

The designed hybrids, NQDA and Cl-NQDA (Figure 1) were synthesized by reacting dopamine (DA) with equimolar ratio of the 1,4-naphthoquinone and 2,3-Dichloro-1,4-naphthoquinone, respectively, using previously reported protocol.[49] The synthesized hybrids were characterized by HPLC, Mass spectrometry and proton NMR spectroscopy (Figure S1-S6, Supporting Information). To investigate the efficacy of the hybrids in modulating the aggregation of α-Syn *in vitro*, we performed various biophysical experiments and DA was used as control.

Inhibition of α-Syn aggregation by the hybrid molecules

The aggregation kinetics of α-Syn in the absence or presence of different molar ratios (α-Syn: tested molecule - 5:1, 1:1, 1:2, 1:3 and 1:5) of the tested molecules was examined by Thioflavin T (ThT) binding assay, a commonly used quantitative method for amyloid formation.[46,50] For α-Syn incubated alone, the ThT signal increased slowly with a lag phase of ~10h and reached a plateau within 40h, indicating the completion of fibrils formation (black curve, Figure 2a and S7). In contrast, the intensity of ThT fluorescence markedly lower upon incubation with DA or the hybrid molecules (Figure 2a,b and S7). DA, at various concentrations delayed the lag phase of α-Syn aggregation by 4-30h, and its maximal inhibition (~60%) of amyloid formation was observed with 1:5 molar ratio of α-Syn: DA (Figure 2b,c and S7a). Similarly, the hybrids inhibited α-Syn aggregation, with prolonged lag phase (of ~15-50h and 13-38h in the presence of NQDA and Cl-NQDA, respectively) indicating dose-dependent inhibitory

effect (Figure 2a-c and S7b). Maximum inhibition was observed at 5-fold molar ratio of the hybrid and at the end of the ThT assay, NQDA and Cl-NQDA inhibited ~88%, and ~76% of amyloid formation, respectively (Figure 2b). Quantitative analysis of the ThT results clearly shows that NQDA was more effective in inhibiting the aggregation of α-Syn, than the other tested molecules (Figure 2b).

The change in secondary conformation of the aggregated α-Syn, in the absence or presence of varied concentrations of the tested molecules, was monitored by CD spectroscopy (Figure S8). α-Syn fibrils alone showed a positive band at ~200 nm and a negative band ~219 nm (black, Figure S8), indicating characteristic β-sheet rich conformation, as reported.[46] Upon co-incubation with increasing doses of the tested molecules, intensity at ~219 nm was reduced in a dose-dependent manner, indicating a decline in β-sheet content (Figure S8).

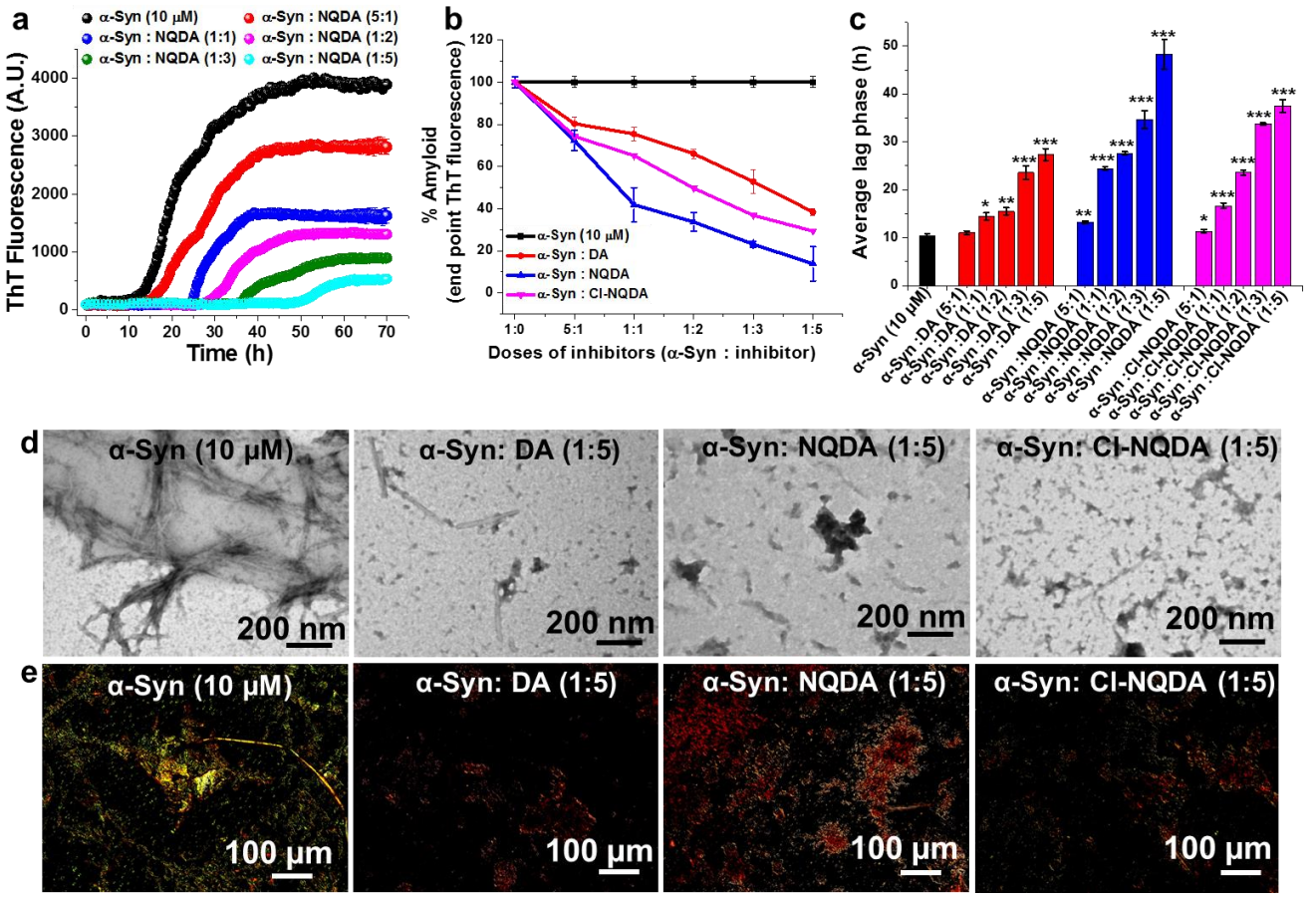


Figure 2. (a) Time-dependent ThT fluorescence assay for the inhibition of α-Syn aggregation (10 μM) in the absence or presence of different molar ratios (α-Syn: NQDA - 5:1, 1:1, 1:2, 1:3 and 1:5) of NQDA. (b) % amyloid remaining in the solution, and (c) average lag-phase, of α-Syn aggregation in the absence or presence of different doses of the tested molecules. (d) TEM, and (e) Congo red stained birefringence images of α-Syn in the absence or presence of 5-fold molar excess of the tested molecules. Experiments were performed in PBS (pH 7.4, 100 mM) at 37 ºC.

The morphology of α-Syn aggregates in the absence or presence of the tested molecules was examined by TEM (Figure 2d and S9). In the absence of tested molecules, α-Syn exhibited long and dense fibrillar network, whereas in the presence of increased doses of the tested molecules the fibrils density was reduced in a dose-dependent manner (Figure 2d and S9). Considerable density of fibrils was detected in the presence of 0.2-, to 3-fold molar excess of DA, however at 5-fold molar excess of DA such fibrils were not noticed, indicating that 5-fold or higher molar excess of DA was required to cause substantial inhibition of α-Syn. In contrast, at 1-fold or higher molar excess of the hybrid molecules no fibrils of α-Syn were detectable, indicating that the hybrid molecules were superior over DA in inhibition of α-Syn aggregation.

Further, we utilized Congo red stained birefringence to corroborate the results described above (Figure 2e and S10). This is a commonly used method to illustrate amyloids, as it shows golden-green birefringence when viewed under cross-polarized light upon binding with amyloids.[51] α-Syn alone showed golden-green birefringence, indicating presence of amyloids (Figure 2e). In the presence of DA, no such birefringence was noted at 5-fold molar ratio but not at lower doses. In contrast, already at 1-fold molar ratio of the hybrid molecules no birefringence was detectable indicating inhibition of fibril formation (Figure 2e and S10).

Comparison of inhibitory efficacy of NQDA with its two constituent molecules

NQDA was found to be more effective in inhibiting the aggregation of α-Syn among the two hybrid molecules, we next examined whether the effect of the hybrid molecules in modulating the aggregation of α-Syn was simply an additive effect of NQ (1,4-naphthoquinone) and DA or presented a synergistic effect due the unique structure of the hybrid. To that end, we have performed aggregation of α-Syn in the absence or presence of different doses (α-Syn: tested molecules – 5:1, 1:1 and 1:5- molar ratio) of NQDA or the two constituent) molecules DA, NQ. ThT results showed that both the constituent molecules inhibited the aggregation of α-Syn in a dose-dependent manner yet at a much lower extent than NQDA (Figure S11). The quantitative ThT measurements revealed that in the presence of 5-fold molar excess of DA, NQ and NQDA, the percentage of α-Syn amyloid remaining in the solution was ~ 35%, 55% and 18% respectively (Figure S11d), suggesting NQDA was more effective in inhibiting α-Syn aggregation than DA or NQ. The superior efficacy of NQDA was observed in all doses tested (Figure S11d). Further, CD results showed that α-Syn alone formed β-sheet rich structure as evident from the positive CD peak at ~ 198 nm and negative peak at ~220 nm (Figure S12). In the presence of all of the

tested molecules the CD intensity at 200 nm was reduced in a dose-dependent manner, yet more reduction of β-sheet content was observed when α-Syn was incubated with NQDA. TEM (Figure S13) and Congo red stained birefringence (Figure S14) results support the conclusion that NQDA was more effective in reduction of amyloid content than the DA and NQ. Collectively, these results suggest that the efficacy of NQDA was exerted from its own structure, i.e., the synergistic effect of both the constituents.

Disruption of preformed fibrils of α-Syn by the hybrid molecules

The mature fibrils and toxic oligomers of α-Syn aggregates in the brain are major risk factors for PD pathogenesis, therefore, reduction of such existing assemblies could be an important avenue for drug development.[6,52,53] To examine the ability of the hybrid molecules to disaggregate preformed fibrils of α-Syn *in vitro*, we first incubated α-Syn (10 μM) alone for 40h to allow its self-aggregation into fibrils (based on the ThT data in Figure 2a, black curve). Then, various doses of the tested molecules (α-Syn: tested molecule - 5:1, 1:1, and 1:5) were added to the preformed fibrils of α-Syn and were further co-incubated for additional 30h. The kinetics of α-Syn fibrils dissociation was monitored by ThT assay (Figure 3a,b and S15), which indicated a decrement of signal with time as the doses of the tested molecules increased, suggesting disruption of preformed fibrils. Maximum disruption was noted at 5-fold molar excess of the tested molecules; DA, NQDA and Cl-NQDA were found to disrupt the preformed fibrils by ~38%, ~68% and ~57%, respectively, compared to untreated α-Syn fibrils (Figure 3b). CD spectra of untreated preformed α-Syn fibrils exhibited a positive band at ~195 nm and a negative band ~218 nm (black, Figure 3c and S12), reflecting a characteristic β-sheet rich conformation. In the presence of the tested molecules, the intensity of CD signal at ~218 nm was reduced in a dose dependent manner (Figure 3c and S16), indicating decrease in β-sheet content reflecting disassembly of the fibrils.

TEM analysis revealed that in the absence of tested molecules, the preformed α-Syn assemblies exhibited typical fibrillar morphology (Figure 3d). In contrast, in the presence of the tested molecules, the density of the fibrillar assemblies was reduced in a dose-dependent manner (Figure 3d and S17). DA was able reduce the preformed fibrils density substantially at 5-fold molar ratio, but not at molar ratios of 0.2- and 1-fold, whereas 1-fold molar ratio of the hybrid molecules was sufficient to markedly reduce the density of the preformed fibrils (Figure 3d and S17a).

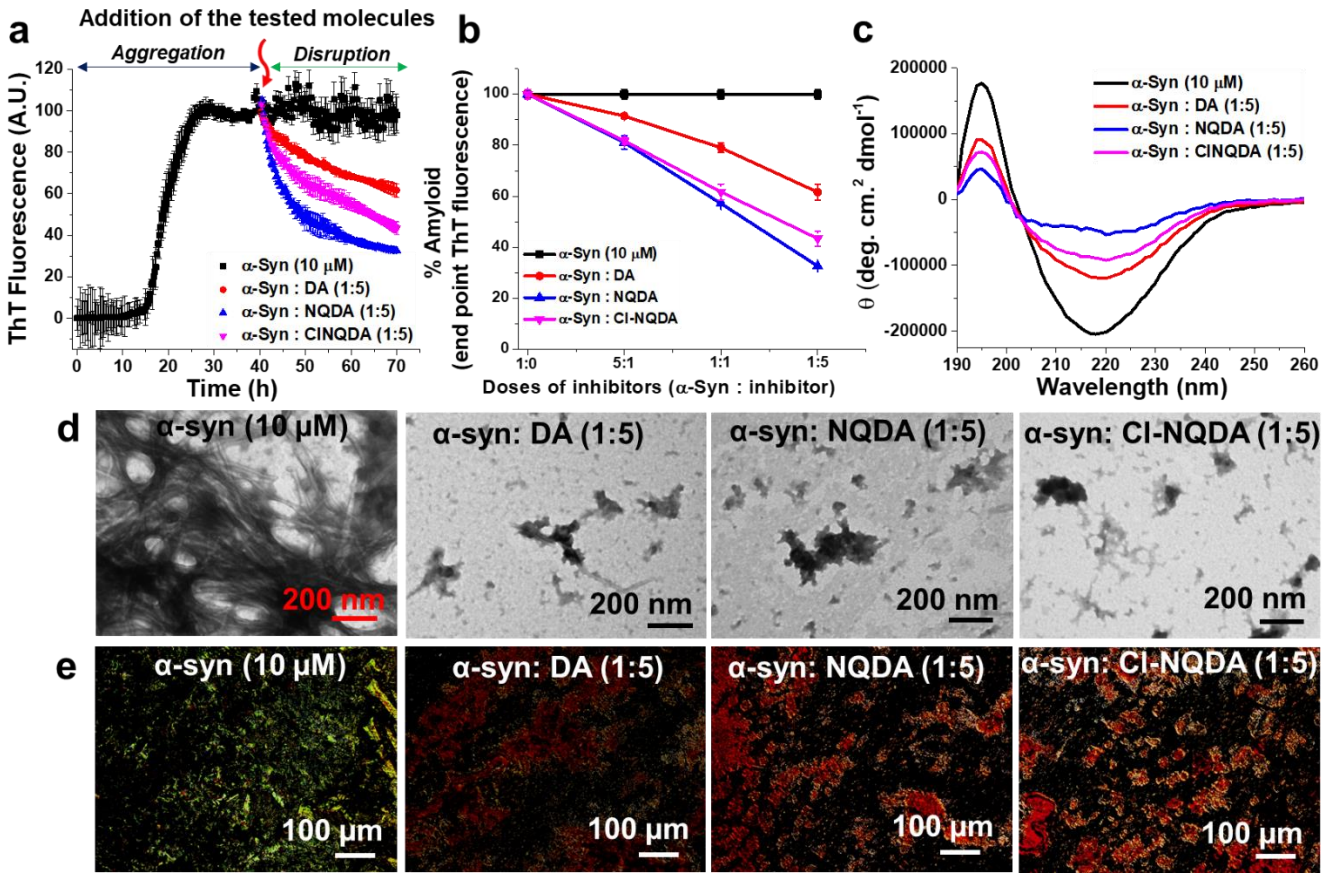


Figure 3. (a) Time-dependent ThT fluorescence assay for the disaggregation of preformed fibrils of α-Syn (10 μM) in the absence or presence of 5-molar excess of the tested molecules. (b) % amyloid remaining in the solution of α-Syn in the absence or presence of different doses of the tested molecules. (c) CD spectra, (d) TEM- and (e) Congo red stained birefringence- images of α-Syn in the absence or presence of 5-fold molar excess of the tested molecules. Experiments were performed in PBS (pH 7.4, 100 mM) at 37 ºC.

Similar results were obtained in Congo red staining birefringence studies. Preformed α-Syn fibrils exhibited golden-green birefringence when incubated alone, indicating presence of amyloids (Figure 3e). In contrast, in the presence 5-fold molar excess of DA and 1-, 5-fold molar excess of the hybrid molecules no such birefringence was observed, suggesting disruption of the preformed fibrils (Figure 3e and S17b).

Collectively, the results of the various *in vitro* assays are in agreement and suggest that the hybrid molecules inhibited α-Syn aggregation efficiently as well as disrupted its preformed fibrillar assemblies. The quantitative ThT data and the other results support the conclusion that NQDA was most effective among the three tested molecules.

Reduction of α-Syn induced cytotoxicity by the hybrid molecules

α-Syn assemblies are believed to exert their neurotoxicity in PD by damaging the cell membrane.[53–55] To evaluate whether the hybrid molecules can reduce the toxicity of α-Syn oligomers and fibrils, we employed two complementary assays, one involving Large Unilamellar Vesicles (LUVs) and the other involving cultured neuronal cells. Monitoring the extent of leakage of the Carboxyfluorescein dye from LUVs loaded with it is a commonly used proxy for damage to cell membrane and cytotoxicity caused e.g. by amyloids.[56–59]

Prior to the leakage assay, LUVs were prepared freshly and their formation was confirmed by TEM (Figure S18). To perform the leakage assay, α-Syn (10 μM) was allowed to aggregate for 10h, in the absence of the tested molecules (NQDA, Cl-NQDA and DA), the time at which α-Syn is assumed to form oligomers, as inferred from the ThT results (black curve, Figure 2a). In parallel, α-Syn (10 μM) was incubated for 10h in the presence of 5-fold molar excess of either one of the tested molecules. After 10h, all the samples were applied to LUVs and dye leakage was monitored by fluorescence assay where % of leakage was calculated using equation SE1 (Supporting Information). The leakage from LUVs treated with Triton X-100 was considered as 100%. Untreated LUVs were monitored to evaluate spontaneous dye leakage. The sample containing α-Syn oligomers (10h aged) in the absence of tested molecules caused leakage of ~45% (red curve, Figure 4a), whereas untreated LUVs caused only ~8% leakage (black curve, Figure 4a). DA, NQDA and Cl-NQDA treated α-Syn oligomer samples caused leakage of ~22%, ~16%, and ~20% respectively (Figure 4a). The lower leakage reflects substantial inhibition of α-Syn oligomer formation by the tested molecules.

To further characterize the disruptive effect of the tested molecules on preformed fibrils of α-Syn (Fig. 3a) we examined whether they were disrupted into toxic oligomers or to a non-toxic species. As control, α-Syn (10 μM) alone was allowed to aggregate for 10h and 70h in the absence tested molecules to generate oligomers and fibrils respectively, as inferred from ThT results (black curve, Figure 2a). Next, the sample containing preformed fibrils was disrupted as described in the ThT assay (Figure 3a), and was used as the experimental sample. Then, LUVs were treated with the different samples. The spontaneous dye leakage from untreated LUVs was ~8% (black curve, Figure 4b); α-Syn oligomers caused ~43% (red curve, Figure 4b) and mature fibrils caused ~22% leakage (blue curve, Figure 4b), indicating that α-Syn oligomers caused more damage to the LUVs than the mature fibrils.[53] In contrast, the preformed fibrils of α-Syn disrupted by DA, NQDA or Cl-NQDA caused less dye leakage of ~19% (magenta curve, Figure 4b), ~13% (green curve, Figure 4b), and ~15% (cyan curve, Figure 4b)

,respectively. These results indicate that the α-Syn preformed fibrillar samples that were treated with the tested molecules caused much lower leakage than untreated oligomers or mature fibrils. This series of experiments suggest that the preformed fibrils of α-Syn were disrupted into non-toxic species which is likely non-oligomeric.

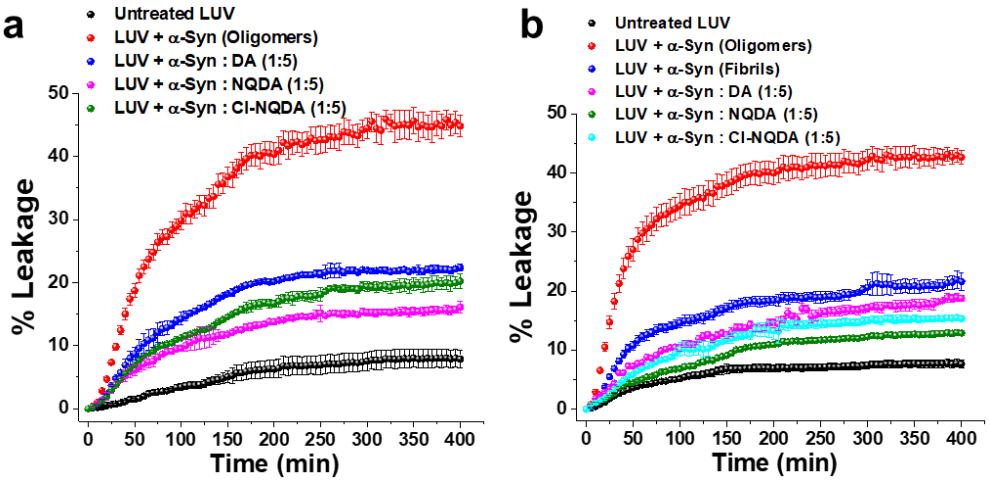


Figure 4. Percentage of dye leakage with time from LUVs treated with α-Syn (a) oligomers and (b) preformed fibrils, in the absence or presence of 5-fold molar excess of the tested molecules. The leakage from LUVs treated with Triton X-100 was considered as 100%.

To examine the effect of the tested molecules on cytotoxicity caused by the α-Syn aggregates, we employed the XTT assay on human neuroblastoma cells lines (SH-SY5Y). First, the cytotoxicity of the tested molecules by themselves was evaluated by incubating them at varied concentrations (1-200 μM) with the cells for 24h and monitoring cell viability (Figure 5). The viability of untreated cells was considered as 100% and 0.5% DMSO was used as vehicle. All three tested molecules exhibited low toxicity towards the cells, and even at highest concentration (200 μM) minimal cell viability was observed, as 94±10%, 87±6% and 83±4% for DA, NQDA and Cl-NQDA, respectively (Figure 5). The cytotoxic effect of α-Syn fibrils, in the absence of the tested molecules, was next examined as a reference (Figure 6). α-Syn alone at varied concentrations (1-20 μM) was incubated for 70h to generate fibrils (as inferred form ThT data, Figure 3a) and the samples were added to the cells, followed by a further incubation period of 24h after which cell viability was recorded. A decrement of cell viability was noted in a dose-dependent manner and ~50% reduction of cell viability (IC_{50}) was observed at ~13 μM. This IC_{50} value was next used for estimating the effect of the tested molecules on α-Syn amyloid-induced cytotoxicity.

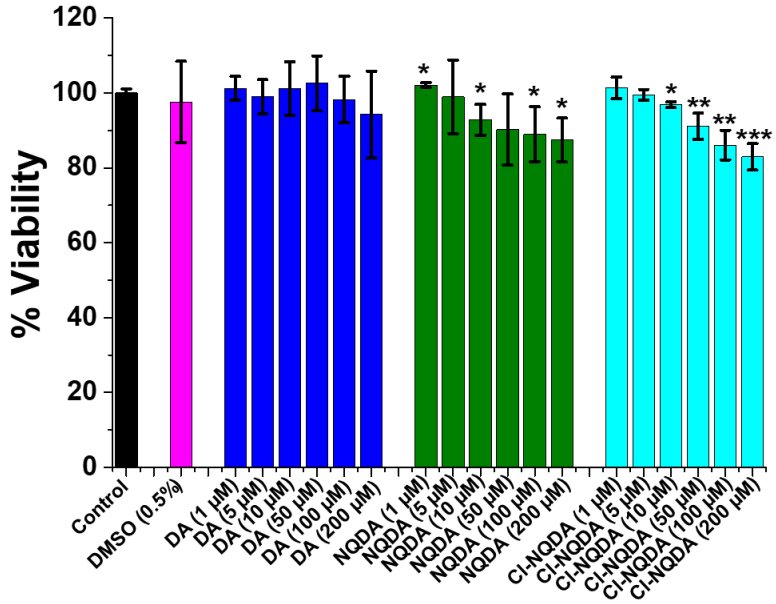


Figure 5. Evaluation of cytotoxicity of DA, NQDA and Cl-NQDA toward SH-SY5Y cells. Cells were incubated with the tested molecules at varied concentrations (1-200 µM) for 24 h and % viability was measured by XTT assay. 0.5% DMSO was used as vehicle to solubilize the tested compounds. Untreated cells were used as control and set to 100% viability. Results are average of 3 independent assays (n = 3 to 6, ±SD) and are expressed as percentage of control cells. Significance (*$p<0.05$), (**$p<0.005$) and (***$p<0.001$).

Two sets of experiments were performed for examine the effect of tested molecules on α-Syn amyloid-induced cytotoxicity. In one set, prior to the addition of different samples to the cells, the tested molecules were co-incubated with α-Syn (13 µM) from time 0 to 70h (similar to the inhibition study describe for the ThT assay). In the other set, the tested molecules were added to the preformed fibrils of α-Syn (40h aged) and were co-incubated for additional 30h (as explain for the disruption study of the ThT assay). Next, the cells were treated for 24h with 13 µM of α-Syn assemblies, alone or together with various concentrations of the tested molecules (Figure 7). Cells treated with α-Syn aggregates that were co-incubated with the tested molecules from time 0, showed enhanced viability which depended on the concentration of the tested molecules. For example, ~71%, ~82% or ~78% viability was noted in the presence of DA, NQDA or Cl-NQDA, respectively at concentration of 65 µM (Figure 7a). Similarly, viability of cells increased upon when treated with preformed α-Syn that had been incubated with the tested molecules in a dose-dependent manner. For instance, 65 µM of DA, NQDA or Cl-NQDA treated samples caused cell viability of ~63%, ~71% or ~70% respectively (Figure 7b). These viability results indicated that the hybrids were efficacious in tumbling the cytotoxicity caused by the α-Syn assemblies, in line with the above described LUVs leakage assay.

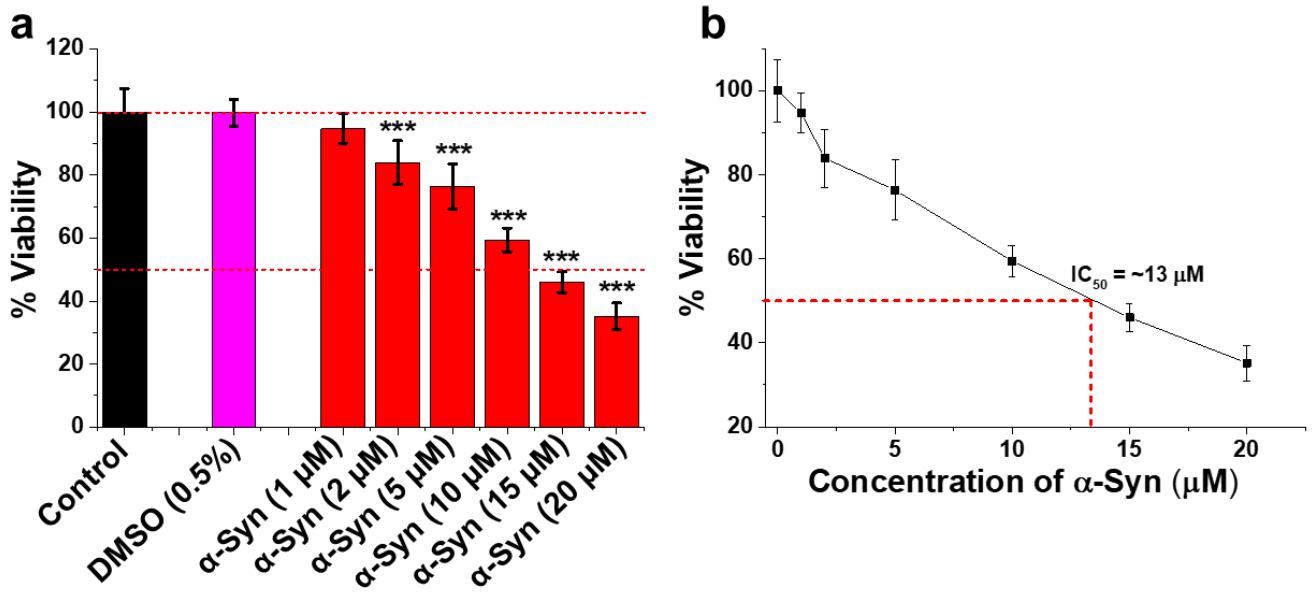


Figure 6. (a) Effect of varied concentrations of α-Syn fibrils on SH-SY5Y cells and (b) the estimation of IC50 value calculated from XTT assay. Confluent cells were incubated with different concentrations of α-Syn fibrils (1-20 μM) for 24h and viability was measured by XTT assay. 0.5 % DMSO was used as vehicle. Untreated cells were used as control and set to 100% viability. **p < 0.05 and ***p < 0.001 compared to untreated samples.

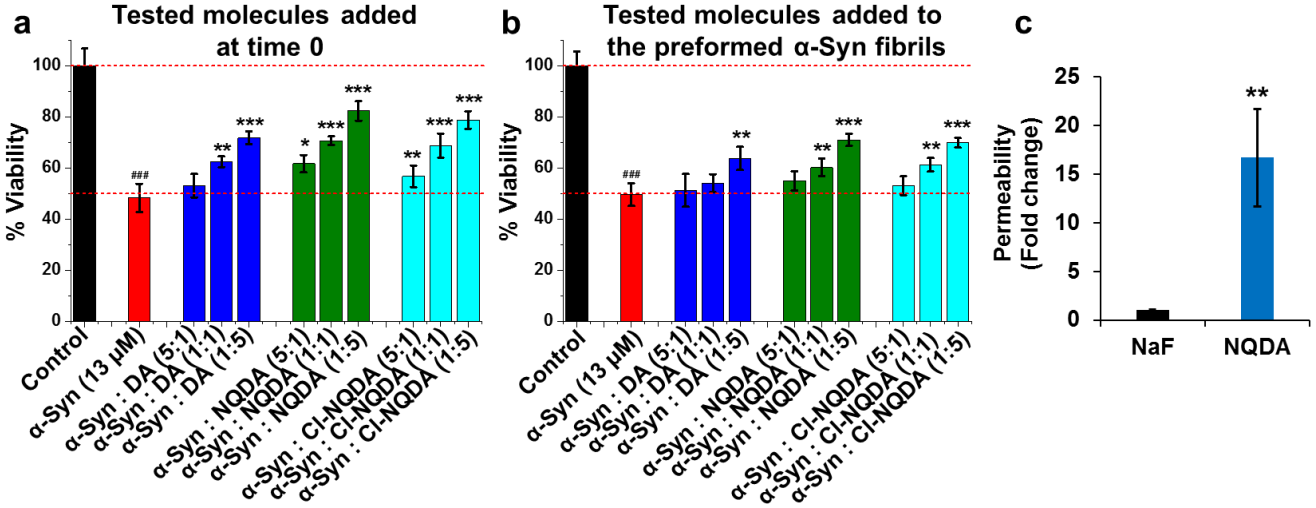


Figure 7. Effects of the tested molecules on α-Syn amyloid induced cytotoxicity. (a) Tested molecules were added to the α-Syn at time 0 and co-incubated for 70h; (b) Tested molecules were added to the preformed fibrils of α-Syn (40h aged) and co-incubated them for additional 30h. Different samples were incubated with SH-SY5Y cells for 24h and the viability was measured by XTT assay. 0.5 % DMSO was used as vehicle and untreated cells were used as control, set to 100% viability. ###p < 0.001 compared to untreated samples. *p < 0.05, **p < 0.005 and ***p < 0.001 compared to the α-Syn fibrils (13 μM). (c) NQDA permeates the BBB *in-vitro*. Permeability of NQDA and sodium fluorescein (NaF) from luminal to abluminal side was measured (n = 4 Transwell inserts per NQDA and n=5 for NaF). Data presented as mean ± SEM. Student's t-test analysis showed **p < 0.01.

NQDA crosses the blood-brain barrier in-vitro

Ability to cross the blood-brain barrier (BBB) is an important attribute for a candidate therapeutic towards neurodegenerative diseases, including PD. To that end, we used an established *in-vitro* model composed of human brain-like endothelial cells (BLECs) together with bovine brain pericytes that closely mimic the *in vivo* BBB.[60] Since, NQDA was found to be more efficient in modulating the aggregation of α-Syn among the tested molecules as observed in the above mentioned combined *in vitro* studies, we then wanted to cheek its ability to cross the BBB. Thus, NQDA or sodium flourescein (NaF) were added at 1.0 mM and 50μM respectively to the luminal compartment of the BBB *in-vitro* model and the permeability was measured as previously described.[61,62] NaF (MW 376 Da) is a paracellular marker widely used to monitor the BBB permeability and treated here as a control. As shown in Figure. 7c, the permeability of NQDA was found to be 16.7-fold higher than NaF which had a Pe value of $18.9\pm5.1x10^{-6}$ cm/sec. The molecular mechanisms involved in this observation is not fully understood and may be investigated in further studies.

Conclusions

We have demonstrated here the ability of Naphthoquinone-Dopamine hybrids, NQDA and Cl-NQDA to inhibit the aggregation of α-Syn using various *in vitro* methods including ThT assay, CD, TEM and Congo red birefringence. These hybrid molecules were also efficacious in disrupting preformed fibrils of α-Syn into non-toxic species as evident from LUVs leakage assay. The hybrid molecules exhibited slight toxicity at high concentration (200 μM) towards human neuronal SH-SY5Y cell lines and markedly ameliorated the cytotoxicity induced by α-Syn fibrils in a dose-dependent manner.

The efficacy of these hybrid molecules can be explained by their ability to bind with α-Syn and disturb its self-assembly process. We propose that the dihydroxyphenyl group of DA within the hybrid molecules may play the key role for binding to α-Syn, possibly through long-range electrostatic interactions. Further, the presence of Naphthoquinone moiety may interfere the α-Syn self-assembly process as observed in previous reports, where that moiety in NQTrp hindered the self-assembly process by amyloidogenic proteins associated in AD, PD and T2DM.[44]

Collectively, our experimental findings accentuate the intriguing nature of these hybrid molecules, i.e. inhibition of amyloid formation as well as disruption of preformed fibrils of α-Syn. These Naphthoquinone-Dopamine hybrids could be a promising scaffold for designing novel therapeutics for PD or other synucleinopathies.

Acknowledgements

This research was supported in part by the Alliance Family Trust (to D.S). Authors thank members of the E.G. and D.S research groups for helpful discussions.

Conflict of interest

The authors declare no conflict of interest.

References

[1] K. A. Jellinger, *Mov. Disord.* **2003**, *18*, 2–12.

[2] C. Peng, R. J. Gathagan, D. J. Covell, C. Medellin, A. Stieber, J. L. Robinson, B. Zhang, R. M. Pitkin, M. F. Olufemi, K. C. Luk, J. Q. Trojanowski, V. M. Y. Lee, *Nature* **2018**, *557*, 558–563.

[3] M. X. Henderson, J. Q. Trojanowski, V. M. Y. Lee, *Neurosci. Lett.* **2019**, *709*, 134316.

[4] V. M. Y. Lee, J. Q. Trojanowski, *Neuron* **2006**, *52*, 33–38.

[5] E. H. Norris, B. I. Giasson, V. M. Y. Lee, *Curr. Top. Dev. Biol.* **2004**, *60*, 17–54.

[6] M. Goedert, *Nat. Rev. Neurosci.* **2001**, *2*, 492–501.

[7] D. W. Dickson, H. Braak, J. E. Duda, C. Duyckaerts, T. Gasser, G. M. Halliday, J. Hardy, J. B. Leverenz, K. Del Tredici, Z. K. Wszolek, I. Litvan, *Lancet Neurol.* **2009**, *8*, 1150–1157.

[8] J. Burré, *J. Parkinsons. Dis.* **2015**, *5*, 699–713.

[9] M. Vilar, H.-T. Chou, T. Luhrs, S. K. Maji, D. Riek-Loher, R. Verel, G. Manning, H. Stahlberg, R. Riek, *Proc. Natl. Acad. Sci.* **2008**, *105*, 8637–8642.

[10] E. A. Mirecka, H. Shaykhalishahi, A. Gauhar, Ş. Akgül, J. Lecher, D. Willbold, M. Stoldt, W. Hoyer, *Angew. Chemie Int. Ed.* **2014**, *53*, 4227–4230.

[11] K. E. Paleologou, G. B. Irvine, O. M. A. El-Agnaf, *Biochem. Soc. Trans.* **2005**, *33*, 1106.

[12] H. Zhang, L.-Q. Xu, S. Perrett, *Methods* **2011**, *53*, 285–294.

[13] M. M. Dedmon, J. Christodoulou, M. R. Wilson, C. M. Dobson, *J. Biol. Chem.* **2005**, *280*, 14733–

14740.

[14] B. Sot, A. Rubio-Muñoz, A. Leal-Quintero, J. Martínez-Sabando, M. Marcilla, C. Roodveldt, J. M. Valpuesta, *Sci. Rep.* **2017**, *7*, 40859.

[15] M. Iljina, L. Hong, M. H. Horrocks, M. H. Ludtmann, M. L. Choi, C. D. Hughes, F. S. Ruggeri, T. Guilliams, A. K. Buell, J.-E. Lee, S. Gandhi, S. F. Lee, C. E. Bryant, M. Vendruscolo, T. P. J Knowles, C. M. Dobson, E. De Genst, D. Klenerman, *BMC Biol.* **2017**, *15*, 57.

[16] D. C. Butler, S. N. Joshi, E. De Genst, A. S. Baghel, C. M. Dobson, A. Messer, *PLoS One* **2016**, *11*, e0165964.

[17] T. Näsström, S. Gonçalves, C. Sahlin, E. Nordström, V. Screpanti Sundquist, L. Lannfelt, J. Bergström, T. F. Outeiro, M. Ingelsson, *PLoS One* **2011**, *6*, e27230.

[18] J. Madine, A. J. Doig, D. A. Middleton, *J. Am. Chem. Soc.* **2008**, *130*, 7873–7881.

[19] M.-G. Choi, M. J. Kim, D.-G. Kim, R. Yu, Y.-N. Jang, W.-J. Oh, *PLoS One* **2018**, *13*, e0195339.

[20] M. Y. Choi, Y. S. Kim, D. Lim, S. J. Kang, Y.-H. Kim, K. Lee, H. Im, *Biochem. Biophys. Res. Commun.* **2011**, *408*, 334–338.

[21] K. Milowska, M. Malachowska, T. Gabryelak, *Int. J. Biol. Macromol.* **2011**, *48*, 742–746.

[22] S. Prabhudesai, S. Sinha, A. Attar, A. Kotagiri, A. G. Fitzmaurice, R. Lakshmanan, R. Lakshmanan, M. I. Ivanova, J. A. Loo, F.-G. Klärner, T. Schrader, M. Stahl, G. Bitan, J. M. Bronstein, *Neurotherapeutics* **2012**, *9*, 464–476.

[23] J. Bieschke, J. Russ, R. P. Friedrich, D. E. Ehrnhoefer, H. Wobst, K. Neugebauer, E. E. Wanker, *Proc. Natl. Acad. Sci. U. S. A.* **2010**, *107*, 7710–5.

[24] M. X, M. LA, F. AL, U. VN, *Parkinsons. Dis.* **2010**, *2010*, 650794–650794.

[25] P. K. Singh, V. Kotia, D. Ghosh, G. M. Mohite, A. Kumar, S. K. Maji, *ACS Chem. Neurosci.* **2013**, *4*, 393–407.

[26] J. Pujols, S. Peña-Díaz, D. F. Lázaro, F. Peccati, F. Pinheiro, D. González, A. Carija, S. Navarro, M. Conde-Giménez, J. García, S. Guardiola, E. Giralt, X. Salvatella, J. Sancho, M. Sodupe, T. F. Outeiro, E. Dalfó, S. Ventura, *Proc. Natl. Acad. Sci. U. S. A.* **2018**, *115*, 10481–10486.

[27] A. Paul, B.-D. Zhang, S. Mohapatra, G. Li, Y.-M. Li, E. Gazit, D. Segal, *Front. Mol. Biosci.* **2019**,

6, 16.

[28] E. J. Bae, H. J. Lee, E. Rockenstein, D. H. Ho, E. B. Park, N. Y. Yang, P. Desplats, E. Masliah, S. J. Lee, *J. Neurosci.* **2012**, *32*, 13454–13469.

[29] S. Spencer, D. Bethea, T. S. Raju, J. Giles-Komar, Y. Feng, *MAbs* **2012**, *4*, 319–25.

[30] P. Sormanni, F. A. Aprile, M. Vendruscolo, *Chem. Soc. Rev.* **2018**, *47*, 9137–9157.

[31] J. Pujols, S. Peña-Díaz, I. Pallarès, S. Ventura, *Trends Mol. Med.* **2020**, *26*, 408–421.

[32] A. C. M. Ferreon, M. M. Moosa, Y. Gambin, A. A. Deniz, *Proc. Natl. Acad. Sci. U. S. A.* **2012**, *109*, 17826–17831.

[33] P. Svenningsson, P. Odin, N. Dizdar, A. Johansson, S. Grigoriou, P. Tsitsi, K. Wictorin, F. Bergquist, D. Nyholm, J. Rinne, F. Hansson, C. Sonesson, J. Tedroff, *Mov. Disord.* **2020**, DOI 10.1002/mds.28020.

[34] Y. A. Sidorova, K. P. Volcho, N. F. Salakhutdinov, *Curr. Neuropharmacol.* **2018**, *17*, 268–287.

[35] O. Hornykiewicz, *Pharmacol. Rev.* **1966**, *18*, 925–964.

[36] J. Drozak, J. Bryła, *Postepy Hig. Med. Dosw. (Online)* **2005**, *59*, 405–20.

[37] K. A. Conway, J. C. Rochet, R. M. Bieganski, J. Lansbury, *Science (80-.).* **2001**, *294*, 1346–1349.

[38] J. Li, M. Zhu, A. B. Manning-Bog, D. A. Di Monte, A. L. Fink, *FASEB J.* **2004**, *18*, 962–964.

[39] M. Bisaglia, L. Tosatto, F. Munari, I. Tessari, P. P. de Laureto, S. Mammi, L. Bubacco, *Biochem. Biophys. Res. Commun.* **2010**, *394*, 424–428.

[40] F. E. Herrera, A. Chesi, K. E. Paleologou, A. Schmid, A. Munoz, M. Vendruscolo, S. Gustincich, H. A. Lashuel, P. Carloni, *PLoS One* **2008**, *3*, e3394.

[41] D. Yedlapudi, G. S. Joshi, D. Luo, S. V. Todi, A. K. Dutta, *Sci. Rep.* **2016**, *6*, 38510.

[42] M. Martinez-Vicente, Z. Talloczy, S. Kaushik, A. C. Massey, J. Mazzulli, E. V. Mosharov, R. Hodara, R. Fredenburg, D. C. Wu, A. Follenzi, W. Dauer, S. Przedborski, H. Ischiropoulos, P. T. Lansbury, D. Sulzer, A. M. Cuervo, *J. Clin. Invest.* **2008**, *118*, 777–778.

[43] R. Scherzer-Attali, R. Shaltiel-Karyo, Y. H. Adalist, D. Segal, E. Gazit, *Proteins* **2012**, *80*, 1962–1973.

[44] G. K. Viswanathan, A. Paul, E. Gazit, D. Segal, *Front. Cell Dev. Biol.* **2019**, *7*, 242.

[45] V. G. KrishnaKumar, A. Paul, E. Gazit, D. Segal, *Sci. Rep.* **2018**, *8*, 71.

[46] M. Frenkel-Pinter, S. Tal, R. Scherzer-Attali, M. Abu-Hussien, I. Alyagor, T. Eisenbaum, E. Gazit, D. Segal, *J. Alzheimers. Dis.* **2016**, *51*, 165–178.

[47] B. Tarus, P. H. Nguyen, O. Berthoumieu, P. Faller, A. J. Doig, P. Derreumaux, *Eur. J. Med. Chem.* **2015**, *91*, 43–50.

[48] D. Latawiec, F. Herrera, A. Bek, V. Losasso, M. Candotti, F. Benetti, E. Carlino, A. Kranjc, M. Lazzarino, S. Gustincich, P. Carloni, G. Legname, *PLoS One* **2010**, *5*, e9234.

[49] M. F. and S. R. PB. Shrestha-Dawadi, S. Bittner, *Synthesis (Stuttg).* **1996**, *12*, 1468–1472.

[50] H. LeVine, *Methods Enzymol.* **1999**, *309*, 274–284.

[51] G. T. Westermark, K. H. Johnson, P. Westermark, *Methods Enzymol.* **1999**, *309*, 3–25.

[52] T. Strohäker, B. C. Jung, S. H. Liou, C. O. Fernandez, D. Riedel, S. Becker, G. M. Halliday, M. Bennati, W. S. Kim, S. J. Lee, M. Zweckstetter, *Nat. Commun.* **2019**, *10*, 1–12.

[53] P. Alam, L. Bousset, R. Melki, D. E. Otzen, *J. Neurochem.* **2019**, *150*, 522–534.

[54] W. Xin, S. Emadi, S. Williams, Q. Liu, P. Schulz, P. He, N. Alam, J. Wu, M. Sierks, W. Xin, S. Emadi, S. Williams, Q. Liu, P. Schulz, P. He, N. B. Alam, J. Wu, M. R. Sierks, *Biomolecules* **2015**, *5*, 1634–1651.

[55] V. Ghiglieri, V. Calabrese, P. Calabresi, *Front. Neurol.* **2018**, *9*, 295.

[56] T. L. Williams, I. J. Day, L. C. Serpell, *Langmuir* **2010**, *26*, 17260–17268.

[57] M. Zhu, J. Li, A. L. Fink, *J. Biol. Chem.* **2003**, *278*, 40186–40197.

[58] C. Fecchio, G. De Franceschi, A. Relini, E. Greggio, M. Dalla Serra, L. Bubacco, P. Polverino de Laureto, *PLoS One* **2013**, *8*, e82732.

[59] S. Kumar, A. Paul, S. Kalita, A. K. Ghosh, B. Mandal, A. C. Mondal, *Chem. Biol. Drug Des.* **2017**, *89*, 888–900.

[60] R. Cecchelli, S. Aday, E. Sevin, C. Almeida, M. Culot, L. Dehouck, C. Coisne, B. Engelhardt, M. P. Dehouck, L. Ferreira, *PLoS One* **2014**, *9*, e99733.

[61] O. Ravid, S. Elhaik Goldman, D. Macheto, Y. Bresler, R. I. De Oliveira, S. Liraz-Zaltsman, F. Gosselet, L. Dehouck, M. S. Beeri, I. Cooper, *Front. Cell. Neurosci.* **2018**, *12*, 359.

[62] G. K. Viswanathan, D. Shwartz, Y. Losev, E. Arad, C. Shemesh, E. Pichinuk, H. Engel, A. Raveh, R. Jelinek, I. Cooper, F. Gosselet, E. Gazit, D. Segal, *Cell. Mol. Life Sci.* **2020**, *77*, 2795–2813.